URTeC: 4043244

A Case Study of Bakken Development Optimization with Complex Constraints

C. Mark Pearson[(1)]; Janz Rondon[(2)]; Stacy Strickland[(1)]; Larry Griffin[(1)]; Dave Ratcliff[(2)]; Garrett Fowler[(2)]
[1.] Liberty Resources, Denver, CO, United States, [2.] ResFrac, Palo Alto, CA, United States.

Abstract

Optimization of unconventional oil and gas assets requires simultaneous consideration of fracturing and porous media flow phenomena. Recent work has demonstrated that a fully coupled fracturing and flow modeling workflow has been used for several recent applications (McClure et al., 2023; Fowler et al., 2023, Pearson et al., 2022). By coupling fracturing and production physics, solutions implicitly reconcile the impact of fracturing designs on depletion results (e.g. - as well spacing is decreased the increased stress shadowing will impact fracture geometries, which in turn, impacts the productivity of the wells). In order to optimize fracturing design for upcoming wells, a coupled model was constructed, calibrated, and used in an optimization workflow.

For this project, a Bakken model was constructed and calibrated to ISIPs, sealed-wellbore pressure monitoring results, bottom hole pressure gauges, and production results from two generations of wells by changing bulk permeability, relative permeability, stress, horizontal toughness, vertical toughness, effective tensile strength, pressure dependent permeability, and time dependent conductivity to match observations of fracture geometry, treating pressure, and three-phase production.

Optimization constraints were set to ensure that all scenarios fell within operational and capital constraints. The optimization was performed in three iterations. The first iteration of scenarios randomly sampled the possible parameter space. Subsequent iterations sampled from parameter-regions that exhibited the highest objective values.

Optimization results demonstrate that there is design optionality. The optimal development design and strategy is a function of the objective function. The biggest parameter driving financial performance is cluster spacing and well spacing. When drilling at closer well spacing there is an improvement in Net Present Value (NPV) per unit at the expense of profitability index (DPI) – all calculated with a 10% discount rate. Fewer wells per drilling section unit increases the DPI, however, comes at a cost to NPV.

The optimization workflow delineates the distinct options available to maximize performance.

Introduction

Field optimization requires consideration of well location (spacing and landing), well completion (stage spacing, perforating and frac design), timing (depletion affects and well-to-well interactions), and economic factors (cost of material and services, commodity prices, etc.). We demonstrate a workflow to assess these factors holistically in the Bakken. The workflow consists of four steps:

1. Pad/area selection.
2. Model calibration to field observations.
3. Model sensitivities to confirm and select the most important design parameters.
4. Model optimization to identify strategies and completion design specifics.

For the study, we employed a fully coupled hydraulic fracture, reservoir, and geomechanics simulator. McClure et al. (2023) describe the simulator:

"The simulator simultaneously solves the equations of fluid flow, proppant transport, water solute transport, fracture mechanics, and poroelasticity in every element in every timestep. Also, the wellbore model includes momentum balance, wellbore friction, perforation pressure-drop, cross-flow of fluid outside casing, and near-wellbore tortuosity."

With respect to this study, the simulator included several functionalities critical to the evaluation of fracturing designs in the Bakken:

- Poroelastic stress calculations: As depletion occurs, there is a commensurate reduction in Shmin (minimum principal stress) in the depleted rock. Consequently, newly created fractures from an adjacent, or infill well, will exhibit bias in the direction of depletion.
- True fracture representation: Fracture elements within the model remain meshed as fractures for the entirety of the simulation. Fractures from an infill well may collide with existing fractures from a parent well, resulting in fluid/proppant exchange between the fractures.
- Integrated economics: The costs associated with any design and revenue associated with production are assigned within the model, allowing for the evaluation of economic metrics such as NPV (net present value) and ROI (return on investment) directly in the model. These metrics can then be set as optimization objectives within an optimization workflow (Kang et al., 2022).

A five well pad, the Arizona pad (Township 158N-93W, Sections 13 & 24), was selected for model calibration. The Arizona pad included calibration data useful for constraining the model, including: offset frac hits, sealed wellbore pressure monitoring (SWPM), production responses from frac hits, and bottomhole pressure responses during frac hits. Additionally, public data was used to guide fracture geometry and production contribution by layer. A single stage from each well was modeled and the production was scaled up accordingly by the number of stages in each respective well.

All five wells were landed in the Middle Bakken formation. The 158-93-13-24-4MBH parent well was drilled and completed first, followed by four child wells drilled and completed 3½ years later. The -5MBH and the -2MBH wells were zipper frac'd first while the -1MBH and -3MBH wells were used for Sealed Wellbore Monitoring (SWPM). One month later, the -1MBH and the -3MBH wells were zipper frac'd. Figure 1 shows the well spacings (along fracture azimuth as well as orthogonal to the wellbores) and the approximate frac dates for each well. The direction of the maximum horizontal stress (Shmax) relative to the wells is ~45 degrees, which increases the 'effective' well spacing and the distance between wells along fracture azimuth.

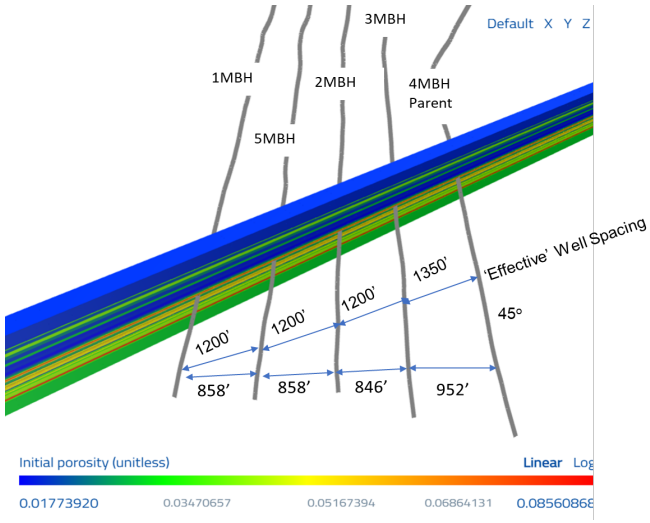

Figure 1. Configuration of calibration wells. The parent well (-4MBH) was completed 3.5 years prior to the infill wells.

History Matching and Model Calibration

Model calibration objectives are separated into five categories, with each category serving as a key observation to match: fracture heights, fracture lengths, treating pressures, cluster efficiency, and production results (including well-to-well interference). Each key observation is detailed below.

Fracture Heights

Middle Bakken fractures are observed to propagate into the Lodgepole (above the Middle Bakken) and into the Three Forks (below) (Liang et al., 2022; Cipolla et al., 2022; and McKimmy et al., 2022). Additionally, water analysis demonstrates that wells with higher water cuts have a significant water contribution from the Birdbear formation (below the Three Forks). Fracture height growth is controlled by the minimum horizontal stress (Shmin) profile. The original Shmin profile was calculated from sonic logs, but the resulting fracture geometry was not consistent with observations. During the history match, Shmin was increased in the Lodgepole and decreased in the Three Forks to yield fracture heights consistent with the production data. Figure 2 shows the final calculated fracture heights.

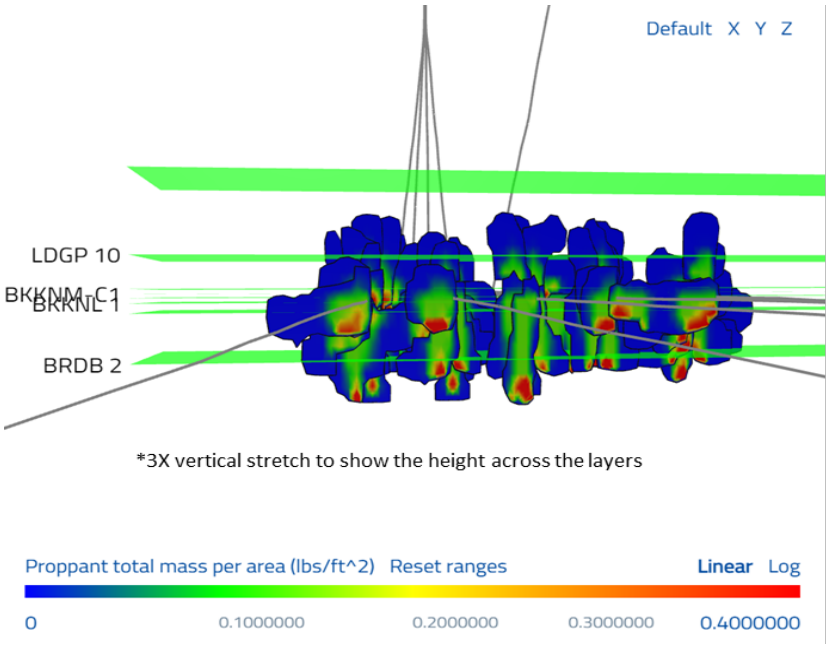

Figure 2 - Fracture growth into the Lodgepole (up) and the Birdbear (down) from wells landed in the Middle Bakken.

Fracture Lengths and Cluster Efficiency

Sealed Wellbore Pressure Monitoring (SWPM) data indicated that fewer than 10% of stages from the -5MBH well hit the -1MBH well, and 50% of the -2MBH stages hit the -3MBH (1200' between each well-pair along fracture azimuth). The -5MBH well was frac'd prior to the -2MBH. The SWPM results suggest that the stress shadowing from the -5MBH fractures push the -2MBH fractures further toward the -3MBH. Further, Figure 3 shows the bottomhole pressure (BHP) gauge in the -4MBH exhibited pressure increases during the fracturing of every stage of the -3MBH (1350' away along fracture azimuth). The pressure hits in the -4MBH are consistent with asymmetric fracture propagation from the -3MBH due to the depletion of the -4MBH. Fracture toughness was elevated slightly from base values to match the observed fracture lengths, suggesting a scale-dependent energy loss (intersection with natural fractures, propagating multiple fracture strands, etc.; McClure et al., 2020). Figure 4 shows the predicted fracture geometries after the -5MBH treatment.

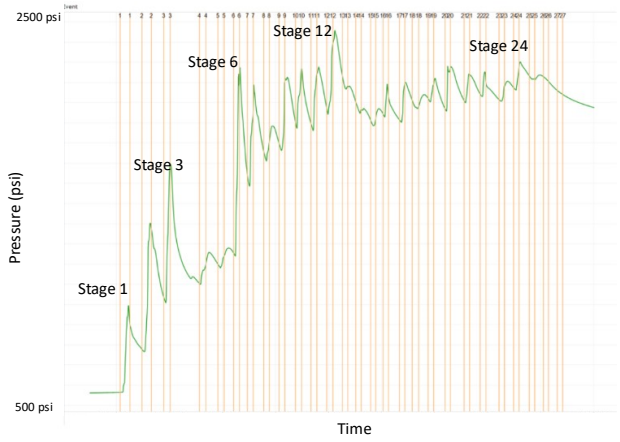

Figure 3 - Frac hits from the closest -3MBH well observed in the parent -4MBH well for all stages

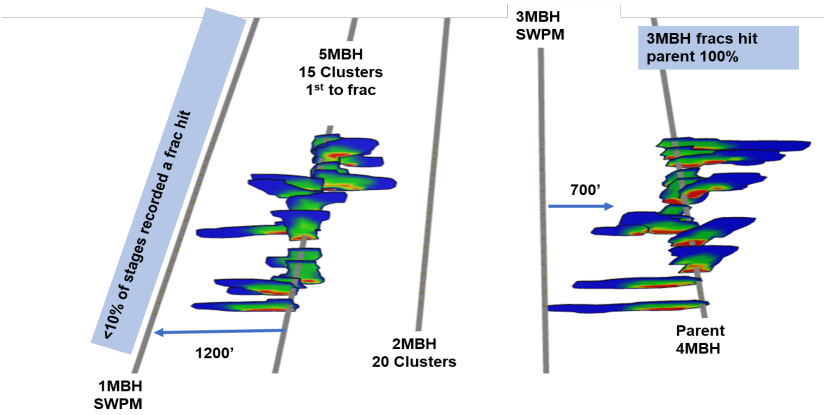

Figure 4 - The resulting fracture geometries showing the proximity of the fractures to each well after tuning the toughness and viscous pressure drop to match geometries.

Figure 5 shows the fracture geometries after the -2MBH treatment. The stress shadow from the -5MBH 'pushes' the fracture further to the right side of the image. Additionally, the -2MBH employed a 20-cluster design with less perforation friction than the 15-cluster design used in the -1MBH, -5MBH, and -3MBH wells. The lower perforation friction in the -2MBH resulted in lower cluster efficiency, also contributing to the relatively longer fractures than in the -5MBH.

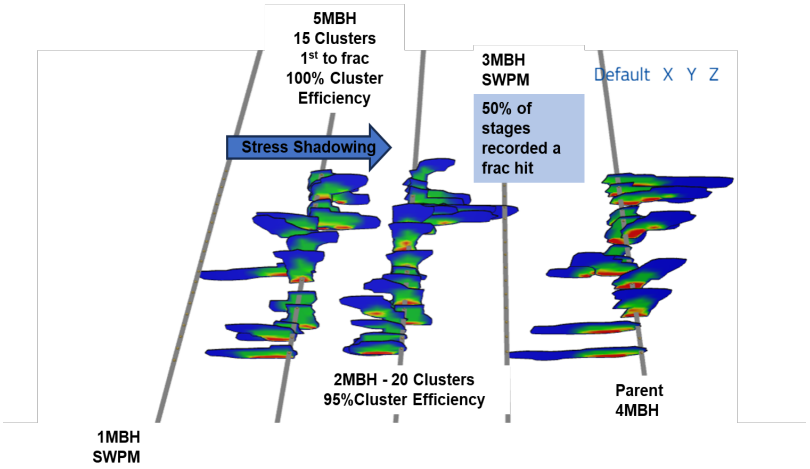

Figure 5 –The -2MBH well exhibits slightly longer fracture lengths than the -5MBH well, consistent with the SWPM data.

Pressure Observations

Initial shut-in pressure (ISIP) observations were used to confirm the magnitude of the Shmin and confirmed that the depletion from the -4MBH parent well did not affect the nearest child well, the -3MBH. ISIP values between 3800-4100 psi were observed for all wells. The initial Shmin profile was shifted approximately 100 psi higher to accommodate these values. Figure 6 shows the distribution ranges for ISIP and the resulting ISIP values from the simulation.

Additionally, it was observed that the ISIP for the well closest to the parent well was not affected by depletion. A lower ISIP value would be anticipated if depletion was present. Combined with the observations of frac hits on the -4MBH well, these ISIPs indicate that the -3MBH well is outside of the depleted region of the -4MBH; however, fractures from the -3MBH well still grow preferentially toward the -4MBH well in the far-field. Figure 6 also shows the extent of depletion at 3.5 years caused by the parent well, and that the values for ISIP for the -3MBH are consistent with the actual values and are unaffected by depletion.

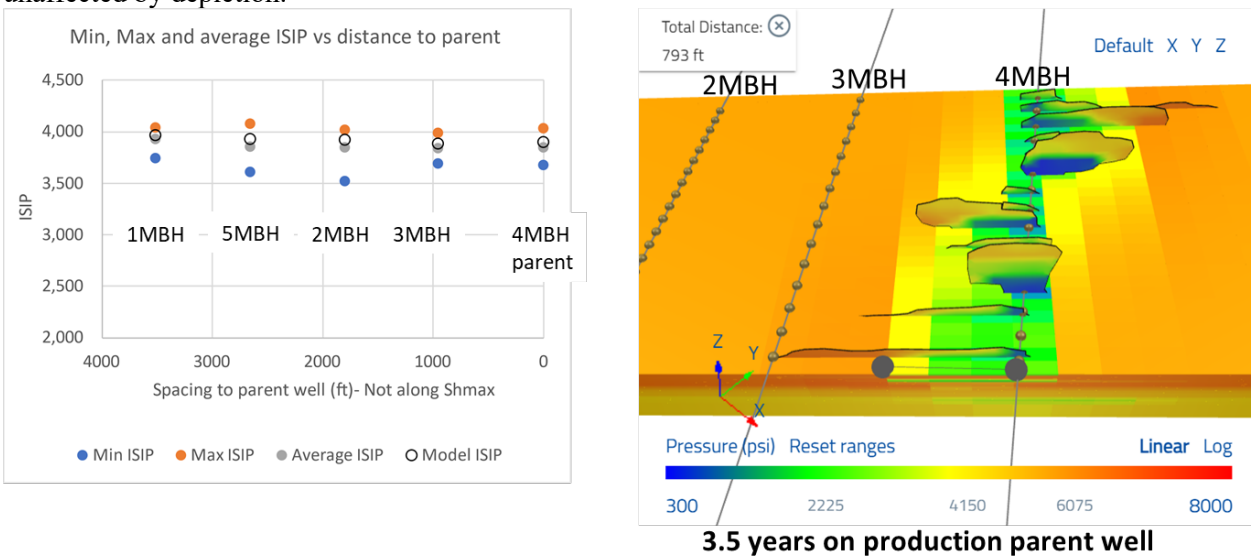

Figure 6 - The pressure plot on the left shows that the depletion from the matrix does not extend from the parent well to the -3MBH well. Additionally, the -3MBH ISIP values are nearly the same as the other wells indicating that the well was drilled in virgin pressure.

Production

Production volumes, gas-oil ratios (GOR), and water cuts were matched for all wells. Additionally, guidance was provided regarding the relative water and oil outputs for each formation layer. Universal adjustments for matrix permeability, relative permeability, and proppant conductivity were tuned to match outputs (i.e., adjustments were made across the entire model domain, not on a well-by-well basis). The -4MBH parent well production was matched first, using calibrated fracture geometries. The bend of the RPI plots were used to guide the reduction in permeability resulting from stress and loss of proppant conductivity. Matching the data required proppant conductivity reduction in excess of that predicted by stress reduction alone, so additional degradation to account for compaction was implemented as a function of time, consistent with prior laboratory studies conducted under Bakken stress conditions (Pearson et al., 2022a; Pearson et al., 2022b; Pearson et al., 2023).

Figures 7 and 8 show the calculated and actual reciprocal productivity index (RPI) plots and cumulative oil production plots for all wells.

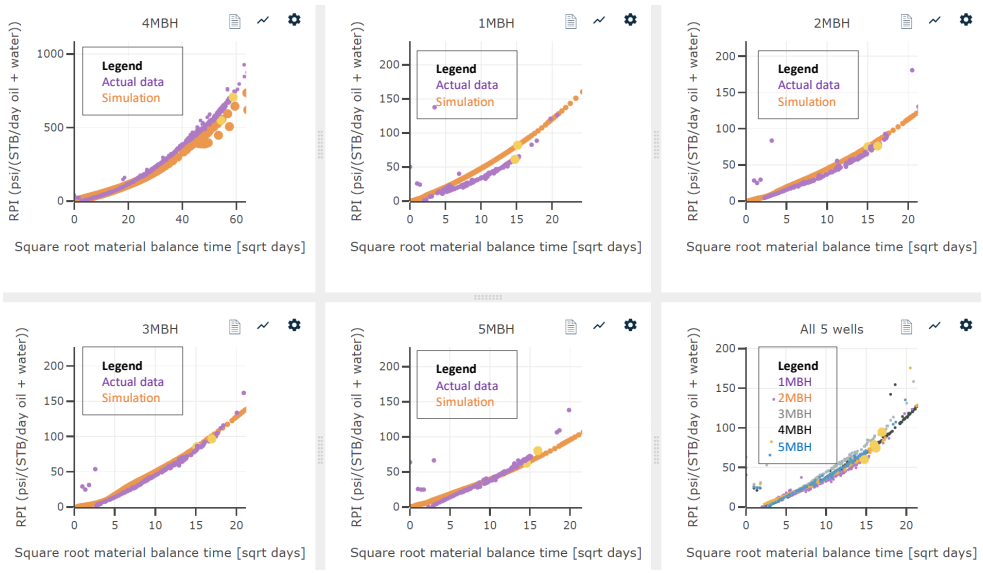

Figure 7 - RPI plots for all 5 wells. Orange dots are simulated values. Purple dots are actual values.

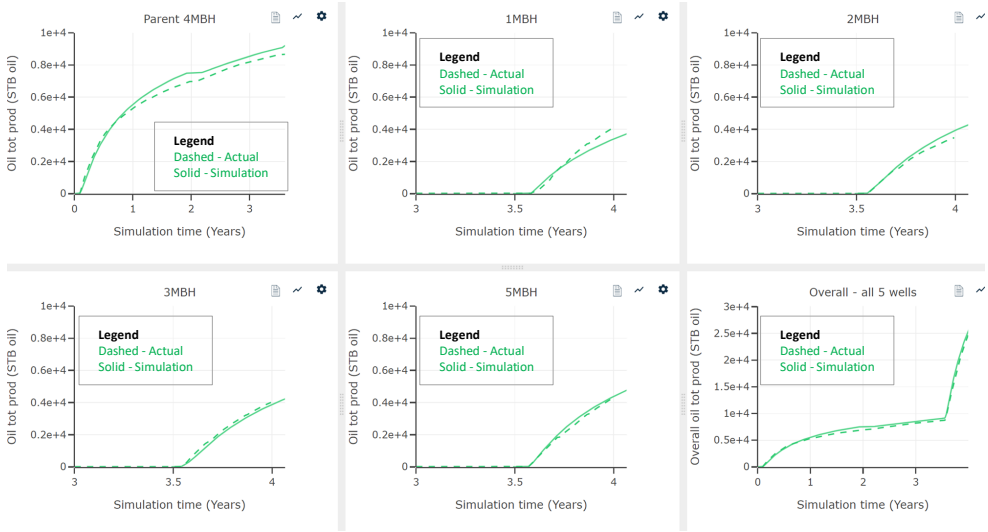

Figure 8 - Resulting total oil production. Dashed lines represent actual data and solid lines are modeled data.

Sensitivity Analysis

The production impact of varying the well spacing, clusters per stage, stage length, size of the frac injection, and drawdown profile was assessed by varying each design parameter independently. The physical settings (geologic, petrophysics, etc.) of the calibrated model are preserved in the sensitivity analysis and held constant. Figure 9 shows the layout of the wells in the base sensitivity model. In all sensitivities, Well P is treated as a parent well with 3.5 years of production prior to the completion of Wells A, B, C, and D.

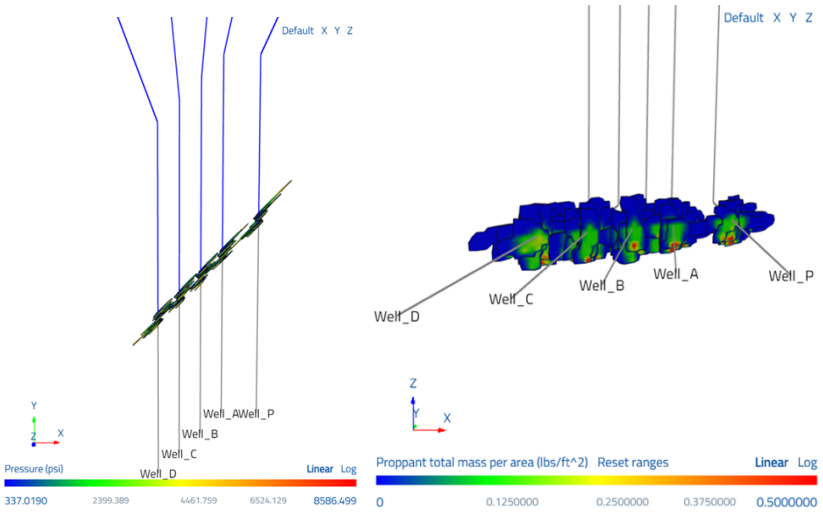

Figure 9 - Hypothetical base model and resulting frac geometry.

Well spacing

The spacing between the four infill wells is tested in a range from 527 to 1320 feet. The well spacing between all the child and parent wells was varied simultaneously. Figure 10 shows that production increases, on a per-well basis, with wider well spacing. Additionally, the impact of decreased well spacing is greater with the time of production, consistent with well-to-well production interference increasing with time.

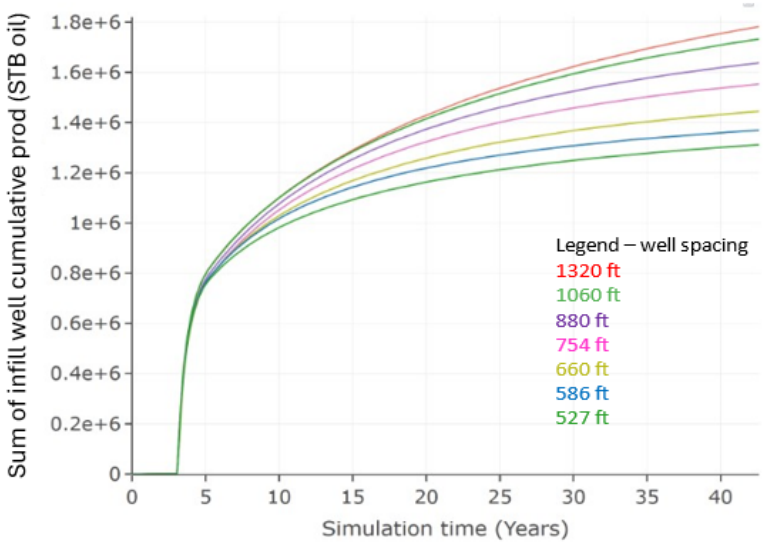

Figure 10: Well productivity increases with wider well spacing. The effect grows through time.

Clusters per stage

Liberty Resources employs an eXtreme Limited Entry (XLE) perforation cluster design strategy (Weddell, et al, 2018). The number of clusters per stage was investigated while maintaining the base stage length, corresponding to a cluster spacing range of 18 to 53 feet. Equal perforation friction was maintained across all simulation cases by keeping the injection rate per cluster constant. Results show increased productivity with denser clusters (more clusters per stage) as shown in Figure 11. The

productivity enhancement is most pronounced in early time, with the EUR of all designs converging at late-time.

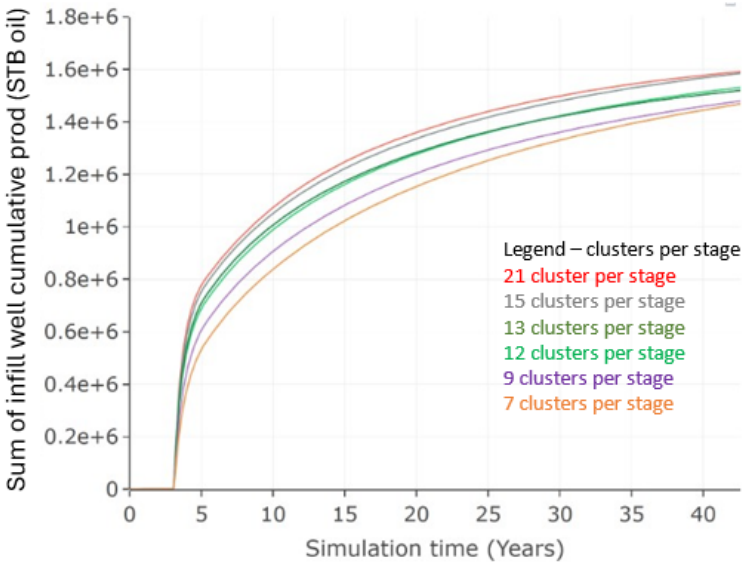

Figure 11. Denser cluster spacing results in higher productivity. All scenarios converge in late-time.

Stage length

Figure 12 shows that as the stage length is increased, the total amount of oil recovered decreases. Additionally, tighter stage lengths are shown to accelerate production earlier in the life of the well.

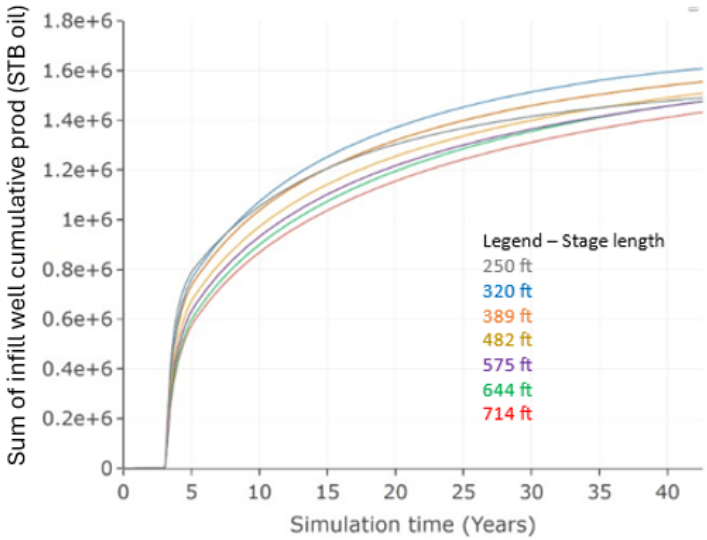

Figure 12 - Production increases with smaller stage length.

Size of frac injection (fluid and proppant increased proportionally)

The size of frac injection was investigating by varying the duration of injection, thus maintaining the same injection rate and proppant concentration. Figure 13 shows an increase in total oil production with larger size of frac injection. The impact of frac size is evident in early-time production, and the difference in productivity is maintained through time.

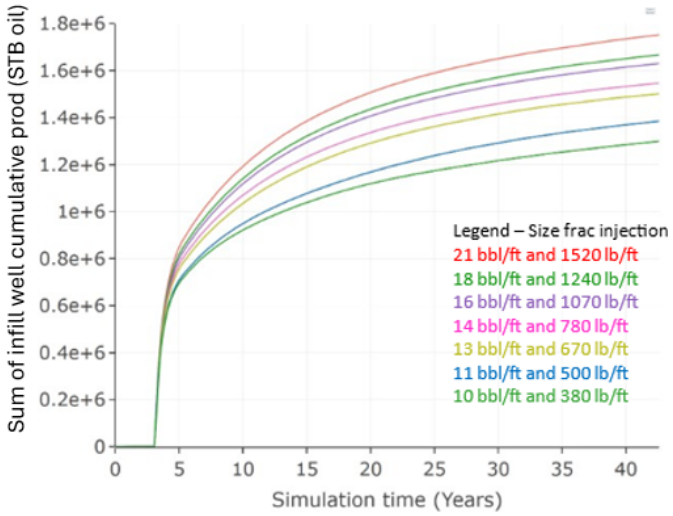

Figure 13 - Increasing the size of the frac (water and proppant proportionally) increases the production of the well.

Larger frac injections also result in higher early-time water cut. Figure 14 shows that larger frac injections result in more fracture area created in the Birdbear formation relative to the Middle Bakken and Three Forks formations. This finding supports the increase in instantaneous water cut with larger size of frac injections as the Birdbear is a water bearing zone.

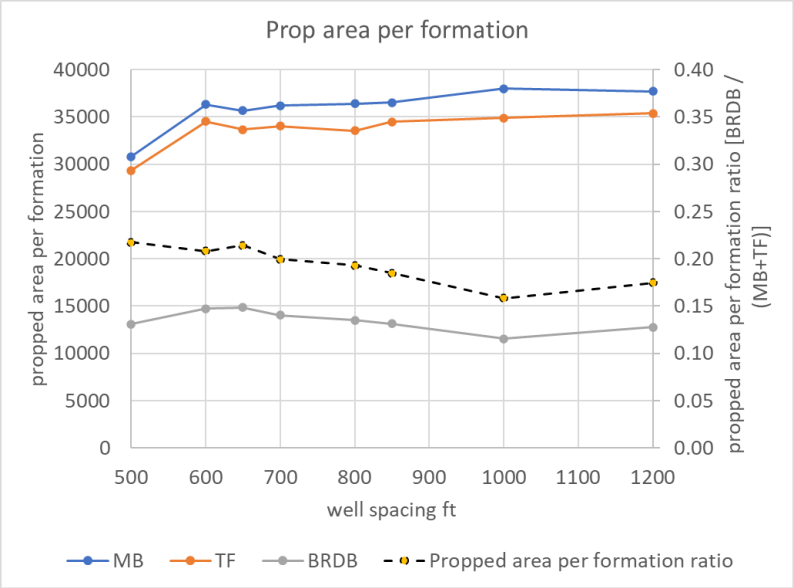

Figure 14 - The propped area in the Birdbear (water bearing formation) increases faster than the overlying Middle Bakken and Three Forks layers when frac size is increased.

Drawdown profile: Figure 15 shows more aggressive drawdown profiles accelerate the oil recoveries in the first 3 years compared to slower drawdowns. However, the cumulative oil trends converge further out in time.

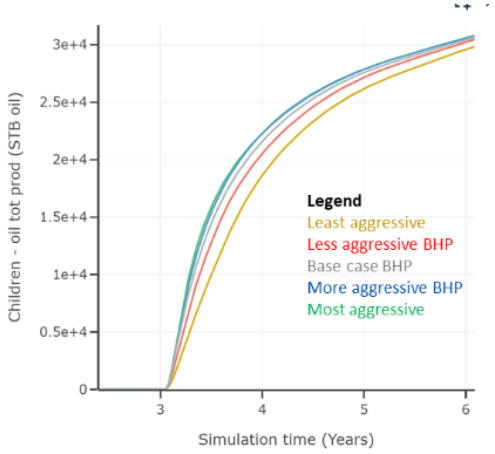

Figure 15 – More aggressive drawdown schedules result in accelerated oil recoveries, but not incremental ultimate recovery.

Economic Optimization

Optimization procedure

The sensitivities demonstrated a range of responses to design changes. To arrive at the economically optimal design, multiple design parameters must be explored in concert and the economic impact of each of those design changes needs to be quantified. A genetic-algorithm optimization procedure was used. The first generation is a space-filling design, sampling all regions of the parameter space (where each design variable is a parameter). Subsequent generations goal-seek the optimal objective value based on the results of the prior generation.

An economic model was incorporated into the base model and tuned using actual costs and revenues of real-world cases. The economic model includes a variety of inputs, including cost of oil, land costs, drilling and completions costs, water disposal costs, facilities and production costs, discount rate, tax rates, etc. Net present value (NPV), discounted return on investment (DROI), and discounted profitability index (DPI) were calculated for every simulation run. DPI (profitability) was the primary economic metric for performing the optimization, and NPV was presented for context in the evaluation.

$$DPI = \frac{DiscountedCumulativeCashFlow}{Discounted\ Cumulative\ CAPEX}$$

$$NPV = \text{CumulativediscountedRevenue} - \text{CumlativediscountedCost}$$

Equations 1 and 2 – Discounted Productivity Index (DPI) and Net Present Value (NPV)

Cases are compared on DPI and NPV normalized to land area, or DPI per DSU (drill spacing unit) and NPV per DSU. One DSU corresponds to a land area of 1 mile by 2 miles.

The three most significant design parameters were chosen for the optimization and varied simultaneously: frac injection size, well spacing, and cluster spacing / stage length. The drawdown profile was fixed for all cases. The proppant and fluid per cluster were varied from 23,000 lbs and 320 bbls per cluster to 33,000 lbs and 476 bbls per cluster. Well spacing was investigated from 480 to 1320 foot spacing, and hereafter is discussed as wells per DSU (11 to 4, respectively). The number of clusters was held constant in all cases, but the stage length was varied from 250’ to 500’, effectively varying the cluster spacing

from 17’ to 34’. Perforation friction was maintained at the same value for all simulations as the number of clusters and perforations per cluster was not changed.

Optimization results

Multiple design parameters were changed revealing a hierarchy of impact in profitability per DSU and showed the largest drivers are well spacing, followed by cluster spacing, and size of frac injection (proppant and fluid).

Firstly, the well spacing is the largest driver of NPV and DPI. DPI per DSU favors fewer wells per DSU, while NPV per DSU favors more wells. Figure 16 shows NPV and DPI per DSU as a function of the number of wells per section for the base frac design (i.e. frac injection size and cluster spacing are kept constant in all scenarios).

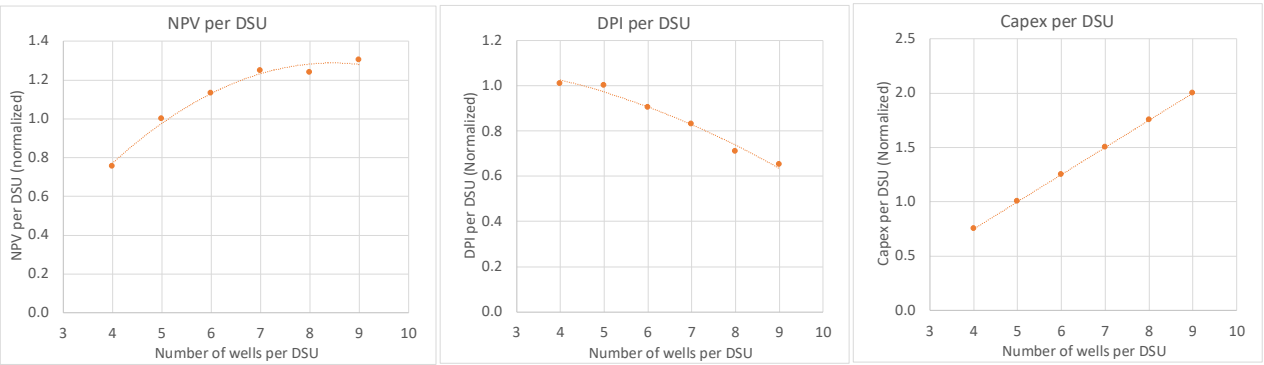

Figure 16. NPV per DSU and DPI per DSU normalized to five wells per DSU.

NPV continues increasing until incremental profit is zero. In Figure 16, we see that NPV per DSU is essentially flat from seven to nine wells per DSU, then decreases at higher well counts. Conversely, DPI is flat from four to five wells per DSU (and then decreases at higher well counts). Because DPI is a measure of capital efficiency it decreases as well-to-well interference increases. Figure 17 shows that there is a negligible interference between wells with either four or five wells per DSU with the base completion design.

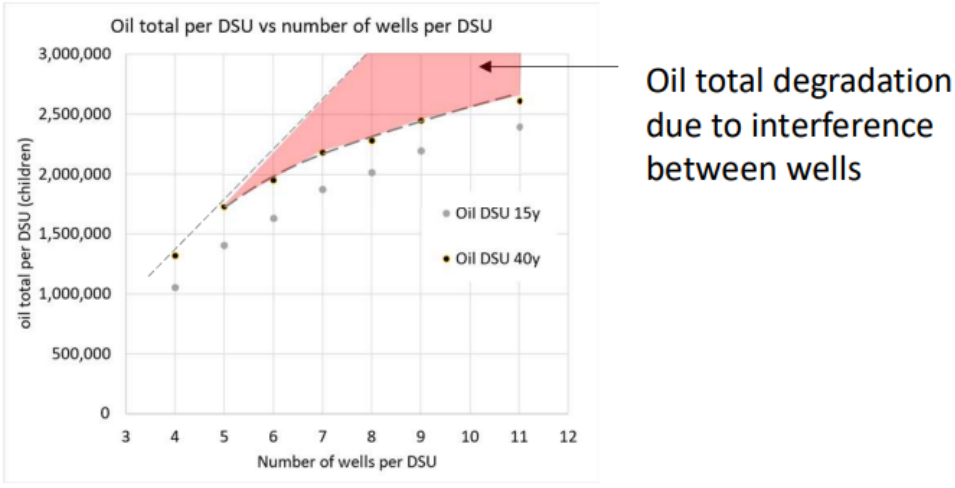

Figure 17. Total DSU oil production as a function of the number of wells per DSU.

The optimal strategy is a function of constraints and objectives. If no alternative investment opportunities exist, a decision maker is likely to optimize for NPV. However, in most cases, alternative investment opportunities *do* exist, and thus a balance of DPI and NPV is a likely decision framework. Additionally, completion design parameters are interdependent. As cluster spacing or frac injection size is changed, the interference at a given well spacing will also change.

The optimization algorithm systemically varied the design parameters, leveraging the interdependencies to optimize DPI per DSU. Figure 18 shows a cross-plot of DPI and NPV from the multiparameter optimization. DPI and NPV are in competition. We observe that DPI is maximized with a lower well count, due to the reduced capital per DSU. NPV is maximized at a higher well count.

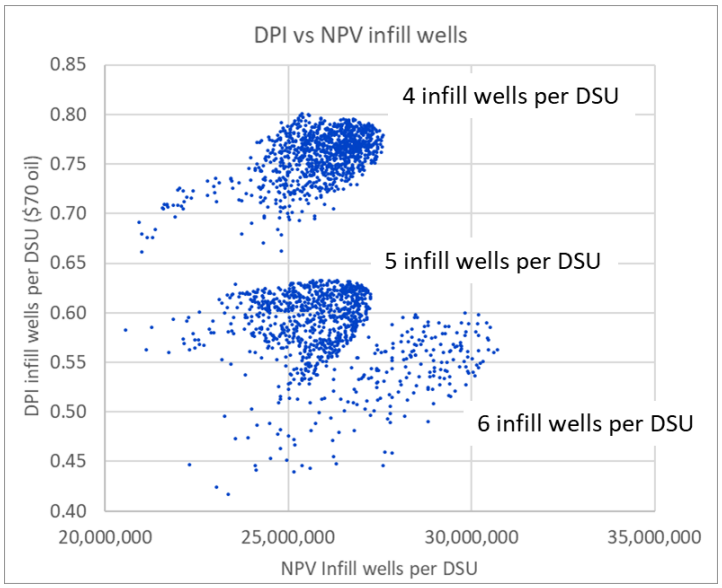

Figure 18. Cross-plot of DPI and NPV per DSU for hundreds of completion scenarios (variable well spacing, frac injection size, and cluster/stage spacing).

Figure 17 shows that well interference occurs at six wells per DSU for the base design. This point of interference remains consistent for the other designs tested. Consequently, the DPI difference between five and six wells per DSU is much larger than the difference between six and seven wells per DSU as DPI is particularly diminished by well-to-well interference (resulting in a lower DPI per DSU as shown in Figure 18).

Secondly, cluster spacing for different well spacing was evaluated. Figure 19 shows the DPI per DSU for hundreds of simulation runs completed during the optimization. We observed that the optimal cluster spacing and well spacing are inversely correlated. As well spacing is increased, there are fewer wells per DSU, and less capital spent drilling wells which results in higher returns to investing in more stages (recall that the number of clusters per stage was kept constant, so tighter cluster spacing corresponds to shorter stages and more total stages per well).

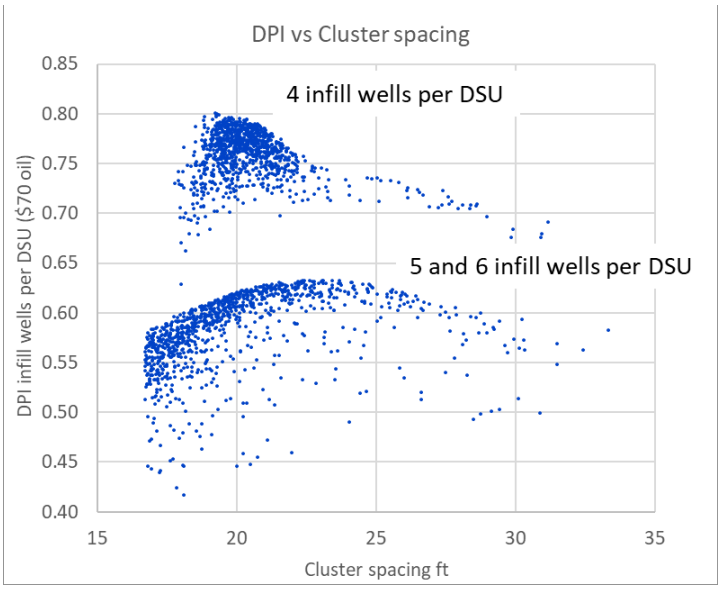

Figure 19. DPI per DSU versus cluster spacing for five and six wells per DSU.

Thirdly, the frac injection size was the third most important design parameter investigated. Figure 20 shows the DPI per DSU versus proppant volume per cluster (correlated with injection volume per cluster). We observe that DPI is less sensitive to frac injection size than cluster/stage spacing and well spacing. Increased injection volumes are associated with increased production as shown in the sensitivities (Figure 13); however, the increased cost associated with the larger volumes offsets the increased revenue from production gains, resulting in flat economic trends. The maximum-DPI versus proppant loading trendlines have been added to Figure 20 to emphasize this result.

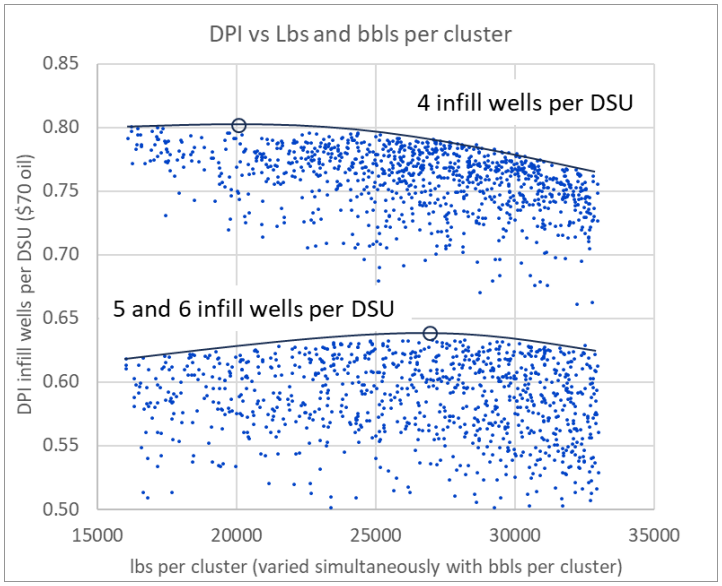

Figure 20. DPI versus lbs of proppant per cluster. Trendlines added for emphasis.

Design Recommendations

Three designs, representing different economic objectives were selected for final consideration. Figure 21 shows these cases on the cross-plot of DPI versus capital expenditure (Capex). The recommended number of wells, cluster spacing, proppant and fluid loadings for each design are summarized in Table 1.

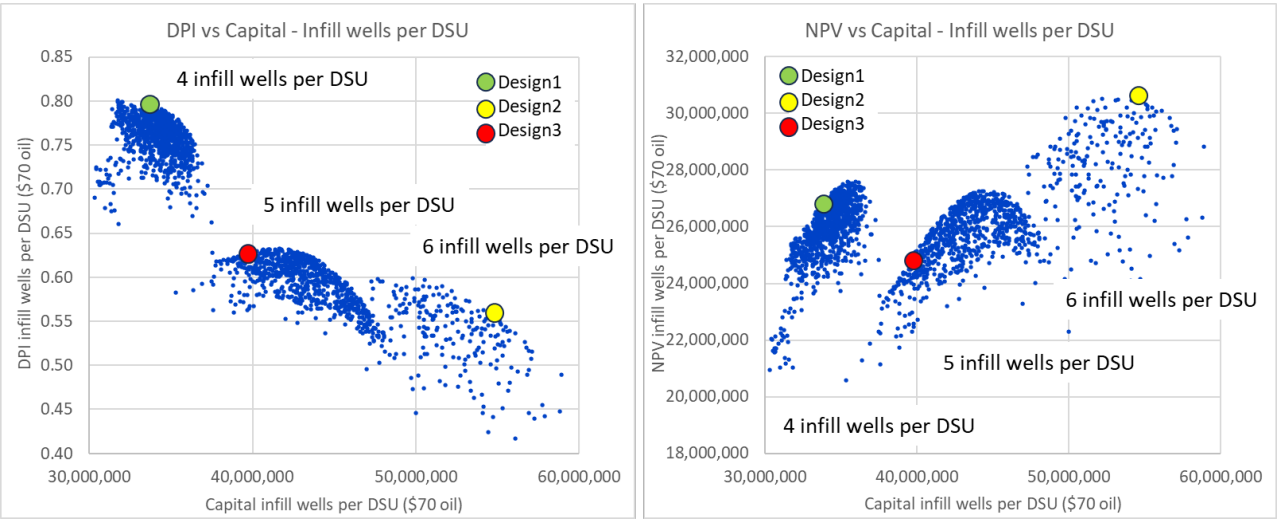

Figure 21. Finalized designs highlighted on DPI versus capex cross-plot.

Design 1 maximizes DPI by reducing from five to four infill wells per DSU. Design 1 comes at the expense of NPV and EUR per DSU.

Design 2 maximizes NPV by using six infill wells per DSU and more stages per well relative to the base design. Design 2 maximizes NPV at the expense of profitability (DPI).

Design 3 maximizes DPI per DSU for the same capital spending per DSU as the operator's current design.

Design	Economic objective	clusters per stage	Cluster spacing (ft)	Size frac lb/cl	Size frac bbl/cl	Stage length	Stages per well	Infill wells per DSU
Base case		15	24.7	23506	380	370	27	5
Design 1	Max DPI per DSU	15	20.1	24356	389	301	33	4
Design 2	Max NPV per DSU	15	19.1	31495	472	286	35	6
Design 3	Max DPI for the same capital spent per DSU	15	22.4	20685	347	335	30	5

Table 1. Three design recommendations for different economic objectives.

The three finalized designs provide for optionality as the objectives and constraints of the operator evolve.

Summary and Conclusions

This study demonstrates an optimization workflow for optimizing well spacing and completion. We utilized a coupled hydraulic fracture and reservoir simulator to ensure that the sensitivity analysis and optimization runs captured the relevant physics and interplay between designs. The key learnings of the study are summarized as follows:

- Coupled hydraulic fracture and reservoir simulation is crucial to capturing the interplay of physics and feedback loops including stress shadowing, well to well interference, and proppant transport.
- The multi-disciplinary approach integrates geology, geomechanics, completions, and reservoir data into a single, consistent model. This approach complicates the calibration process as changing a parameter, such as permeability, affects all aspects of the model (leak-off as well as

production). However, non-unique aspects of the models are reduced, though not eliminated, ultimately increasing the robustness of the model.

- Model confidence is increased with calibration data. By incorporating key diagnostics in the model calibration, model predictions were verified with a broad range of field observations.
- Key stimulation design parameters, such as well spacing, cluster/stage spacing, and injection volumes cannot be optimized individually, but must be simultaneously optimized.
- The optimization reveals that different completion designs optimize different economic objectives, providing optionality.
- The ranking of designs is a function of the economic assumptions used within the analysis. Changes to oil price, operating costs, or discount rate will change the ranking of the various designs. For instance, Figure 22 shows NPV and DPI as a function of discount rate. As discount rate is increased, future revenues are worth less and initial capital expense weighs more heavily on the optimization. Consequently, higher discount rates shift the NPV-optimum to fewer wells and increases relative DPI benefit of five wells per DSU.

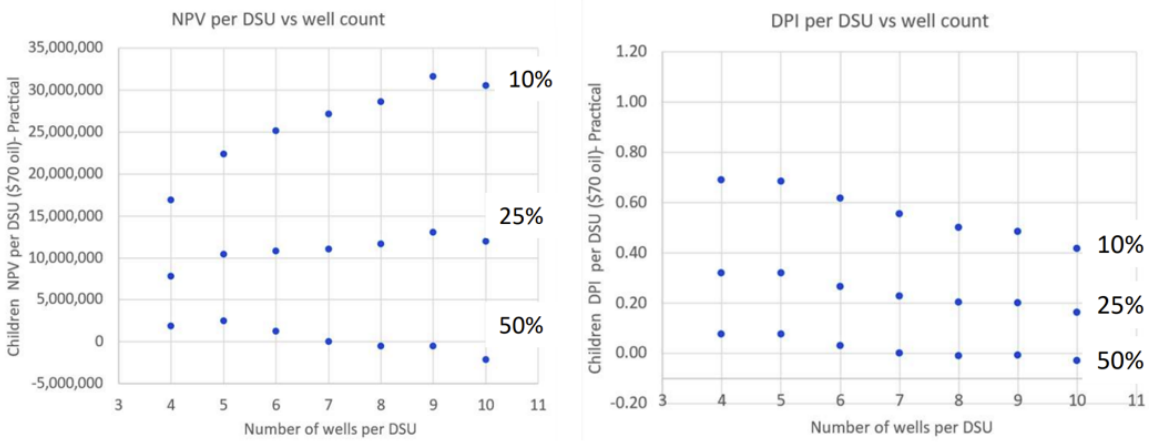

Figure 22. NPV and DPI as a function of the number of wells per DSU for various discount rates.

References

Cipolla, Craig, Wolters, Jennifer, McKimmy, Michael, Miranda, Carlos, Hari-Roy, Stephanie, Kechemir, Aicha, and Nupur Gupta. "Observation Lateral Project: Direct Measurement of Far-Field Drainage in the Bakken." *SPE Prod & Oper* 38 (2023): 20–34. doi: https://doi.org/10.2118/209164-PA

Fowler, G. J., McClure, M. W., Singh, A., Irvin, R., Ratcliff, D., Ponners, C., and J. Rondon. "Case Studies in Integrated Fracture Design and Well Spacing Optimization in Shale." Paper presented at the International Petroleum Technology Conference, Dhahran, Saudi Arabia, February 2024. doi: https://doi.org/10.2523/IPTC-24396-MS

Kang, Charles A., McClure, Mark W., Reddy, Somasekhar, Naidenova, Mariyana, and Zdravko Tyankov. "Optimizing Shale Economics with an Integrated Hydraulic Fracturing and Reservoir Simulator and a Bayesian Automated History Matching and Optimization Algorithm." Paper presented at the SPE Hydraulic Fracturing Technology Conference and Exhibition, The Woodlands, Texas, USA, February 2022. doi: https://doi.org/10.2118/209169-MS

Liang, Y., Meier, H. et al., 2022. Accelerating Development Optimization in the Bakken Using an Integrated Fracture Diagnostic Pilot. Paper presented at the SPE/AAPG/SEG Unconventional Resources

Technology Conference, Houston, Texas, USA, June 2022. doi: https://doi.org/10.15530/urtec-2022-3719696

McClure, Mark, Albrecht, Magdalene, Bernet, Carl, Cipolla, Craig, Etcheverry, Kenneth, Fowler, Garrett, Fuhr, Aaron, Gherabati, Amin, Johnston, Michelle, Kaufman, Peter, MacKay, Mason, McKimmy, Michael, Miranda, Carlos, Molina, Claudia, Ponners, Christopher, Ratcliff, Dave, Rondon, Janz, Singh, Ankush, Sinha, Rohit, Sung, Anthony, Xu, Jian, Yeo, John, and Rob Zinselmeyer. "Results from a Collaborative Industry Study on Parent/Child Interactions: Bakken, Permian Basin, and Montney." Paper presented at the SPE Hydraulic Fracturing Technology Conference and Exhibition, The Woodlands, Texas, USA, January 2023. doi: https://doi.org/10.2118/212321-MS

McClure, Mark , Picone, Matteo , Fowler, Garrett , Ratcliff, Dave , Kang, Charles , Medam, Soma , and Joe Frantz. "Nuances and Frequently Asked Questions in Field-Scale Hydraulic Fracture Modeling." Paper presented at the SPE Hydraulic Fracturing Technology Conference and Exhibition, The Woodlands, Texas, USA, February 2020. doi: https://doi.org/10.2118/199726-MS

McKimmy, Michael, Hari-Roy, Stephanie, Cipolla, Craig, Wolters, Jennifer, Jackson, Haffener, and Haustveit Kyle. "Hydraulic Fracture Geometry, Morphology, and Parent-Child Interactions: Bakken Case Study." Paper presented at the SPE Hydraulic Fracturing Technology Conference and Exhibition, The Woodlands, Texas, USA, February 2022. doi: https://doi.org/10.2118/209162-MS

Pearson, C. Mark, and Garrett Fowler. "The Impact of Extended-Time Proppant Conductivity Impairment on the Ultimate Recovery from Unconventional Horizontal Well Completions." Paper presented at the SPE International Hydraulic Fracturing Technology Conference & Exhibition, Muscat, Oman, January 2022. doi: https://doi.org/10.2118/205294-MS

Pearson, C. Mark, Green, Christopher A., McGill, Mark, and David Milton-Tayler. "Extended-Time Conductivity Testing of Proppants Used for Multi-Stage Horizontal Completions." Paper presented at the SPE International Hydraulic Fracturing Technology Conference & Exhibition, Muscat, Oman, January 2022. doi: https://doi.org/10.2118/205272-MS

Pearson, C. Mark, Green, Christopher A., Milton-Tayler, David, and Viviana Trevino. "Extended-Time Conductivity Testing of Proppants at 0.5 lb/ft^2 Used for Slickwater Multi-Stage Horizontal Completions." Paper presented at the SPE Hydraulic Fracturing Technology Conference and Exhibition, The Woodlands, Texas, USA, January 2023. doi: https://doi.org/10.2118/212334-MS

Weddle, P., Griffin, L., & Pearson, C. M. (2018, January 23). Mining the Bakken II – Pushing the Envelope with Extreme Limited Entry Perforating. Society of Petroleum Engineers. doi: https://doi.org/10.2118/189880-MS